

Reactivity of $Y_3(OR)_7Cl_2(THF)_2$ with Organoaluminum Reagents: Formation of the Yttrium–Aluminum Complexes $Y(OR)_3(AlMe_3)_3$, $Y(OR)_3(AlMe_3)_2(THF)$, and $Y(OR)_3(AlMe_2)Cl(THF)_2$ and the Halides $YCl_3(DME)_2$ and $YCl_3(THF)_3Y_3(OR)_7O$ ($R = CMe_3$)¹

William J. Evans,* Timothy J. Boyle, and Joseph W. Ziller

Contribution from the Department of Chemistry, University of California, Irvine, California 92717

Received September 28, 1992

Abstract: The trimetallic structure of $Y_3(OCMe_3)_7Cl_2(THF)_2$ (**1**), which is typically retained in reactions of yttrium *tert*-butoxide complexes, was easily disrupted by trimethylaluminum to generate a series of mixed-metal yttrium–aluminum compounds. **1** reacted with $AlMe_3$ in hexanes to form $Y[(\mu-OCMe_3)(\mu-Me)AlMe_2]_3$ (**2**), $(Me_3CO)(THF)Y[(\mu-OCMe_3)(\mu-Me)AlMe_2]_2$ (**3**), and $(Me_3CO)(Cl)(THF)_2Y[(\mu-OCMe_3)_2AlMe_2]$ (**4**). **2** crystallized from hexanes in the space group $P31c$ with $a = 15.842(2)$ Å, $c = 7.9994(14)$ Å, $V = 1738.6(4)$ Å³, and $D_{\text{calcd}} = 1.002$ Mg/m³ for $Z = 2$. Least-squares refinement of the model based on 799 reflections ($|F_o| > 4.0\sigma|F_o|$) converged to a final $R_F = 9.9\%$. **2** can be viewed as a tris(trimethylaluminum) adduct of $Y(OCMe_3)_3$, a unit which has not previously been isolated in a monometallic form. An octahedral coordination environment around the yttrium in **2** was generated by three doubly-bridging $[(\mu-OCMe_3)(\mu-Me)AlMe_2]$ moieties which contain tetrahedrally-coordinated aluminum. **3** crystallized from toluene in the space group $Pca2_1$ with $a = 14.408(4)$ Å, $b = 17.216(3)$ Å, $c = 12.186(2)$ Å, $V = 3022.7(11)$ Å³, and $D_{\text{calcd}} = 1.153$ Mg/m³ for $Z = 4$. Least-squares refinement of the model based on 1848 reflections ($|F_o| > 3.0\sigma|F_o|$) converged to a final $R_F = 4.5\%$. The six-coordinate octahedral environment around yttrium in **3** is similar to that of **2**, except that THF and a terminal *tert*-butoxide ligand have replaced one of the three $[(\mu-OCMe_3)(\mu-Me)AlMe_2]$ units. **4** crystallized from THF/DME (20:1) in space group $Pnma$ with $a = 19.752(25)$ Å, $b = 12.765(28)$ Å, $c = 11.938(10)$ Å, $V = 3010(8)$ Å³, and $D_{\text{calcd}} = 1.09$ Mg/m³ for $Z = 4$. Only one chelating aluminum moiety is present in the octahedral coordination sphere of **4**, and it differs from those in **2** and **3** in that it contains two bridging *tert*-butoxide ligands and two terminal methyl groups. $YCl_3(DME)_2$ (**5**) was also obtained from the **1**/ $AlMe_3$ reaction mixture by crystallization from THF/DME (3:1). **5** crystallized in space group $P2_1/c$ with $a = 11.343(5)$ Å, $b = 8.855(3)$ Å, $c = 15.617(9)$ Å, $\beta = 104.59(4)^\circ$, $V = 1518.1(12)$ Å³, and $D_{\text{calcd}} = 1.64$ Mg/m³ for $Z = 4$. Least-squares refinement of the model based on 1659 reflections ($|F_o| > 3.0\sigma|F_o|$) converged to a final $R_F = 3.2\%$. The seven-coordinate complex adopts a distorted pentagonal bipyramidal geometry with chloride ions in the axial positions. The reaction of $LiAlMe_4$ with $Y_3(OCMe_3)_7Cl_2(THF)_2$ generated the tetrametallic complex $[(THF)_3Y(\mu-Cl)_3]Y_3(\mu-OCMe_3)_3(\mu-OCMe_3)_3(\mu-O)$ (**6**). **6** crystallized from toluene in the space group $R\bar{3}$ with $a = 14.615(3)$ Å, $c = 50.993(12)$ Å, $V = 9433(3)$ Å³, and $D_{\text{calcd}} = 1.274$ Mg/m³ for $Z = 6$. Least-squares refinement of the model based on 1344 reflections ($|F_o| > 6.0\sigma|F_o|$) converged to a final $R_F = 7.8\%$. **6** can be viewed as a $YCl_3(THF)_3$ unit attached to a trimetallic yttrium *tert*-butoxide complex similar to **1**. The complex contains a tetrahedral arrangement of yttrium atoms surrounding an internal μ_4 -oxide ligand, and the yttrium trichloride unit is seven-coordinate as in **5**.

Introduction

Recent studies of the chemistry of alkoxide complexes of yttrium and the lanthanide metals have shown that this combination of metals and ligands prefers to form polymetallic species^{2–12} except

when very bulky alkoxides are involved.^{13–17} For example, with isopropoxide ligands, pentametallic and hexametallic species of

(1) Reported in part at the 203rd National Meeting of the American Chemical Society, San Francisco, CA, April 1992; see Abstract INOR 702.

(2) Caulton, K. G.; Hubert-Pfalzgraf, L. G. *Chem. Rev.* **1990**, *90*, 969–995.

(3) Andersen, R. A.; Templeton, D. H.; Zalkin, A. *Inorg. Chem.* **1978**, *17*, 1962–1964.

(4) Evans, W. J.; Sollberger, M. S.; Hanusa, T. P. *J. Am. Chem. Soc.* **1988**, *110*, 1841–1850.

(5) Evans, W. J.; Sollberger, M. S. *Inorg. Chem.* **1988**, *27*, 4417–4423.

(6) (a) Bradley, D. C.; Chudzynska, H.; Frigo, D. M.; Hursthouse, M. B.; Mazid, M. A. *J. Chem. Soc., Chem. Commun.* **1988**, 1258–1259. (b) Bradley, D. C.; Chudzynska, H.; Frigo, D. M.; Hammond, M. E.; Hursthouse, M. B.; Mazid, M. A. *Polyhedron* **1990**, *9*, 719–726.

(7) Poncelet, O.; Sartain, W. J.; Hubert-Pfalzgraf, L. G.; Folting, K.; Caulton, K. G. *Inorg. Chem.* **1989**, *28*, 263–267.

(8) Wu, J.; Boyle, T. J.; Shreeve, J. L.; Ziller, J. W.; Evans, W. J. *Inorg. Chem.* **1993**, *32*, 1130–1134.

(9) Bradley, D. C.; Chudzynska, H.; Hursthouse, M. B.; Motevalli, M. *Polyhedron* **1991**, *10*, 1049–1059.

(10) Evans, W. J.; Shreeve, J. L.; Ziller, J. W. Manuscript in preparation.

(11) (a) See also: Evans, W. J.; Sollberger, M. S. *J. Am. Chem. Soc.* **1986**, *108*, 6095–6096. (b) Schumann, H.; Kociok-Kohn, G.; Loebel, J. Z. *Anorg. Allg. Chem.* **1990**, *581*, 69–81.

(12) Poncelet, O.; Hubert-Pfalzgraf, L. G.; Daran, J.-C.; Astier, R. *J. Chem. Soc., Chem. Commun.* **1989**, 1846–1848.

(13) Stecher, H. A.; Sen, A.; Rheingold, A. L. *Inorg. Chem.* **1989**, *28*, 3280–3282.

(14) Hitchcock, P. B.; Lappert, M. F.; MacKinnon, I. A. *J. Chem. Soc., Chem. Commun.* **1988**, 1557–1558.

(15) Evans, W. J.; Golden, R. E.; Ziller, J. W. *Inorg. Chem.* **1991**, *30*, 4963–4968.

(16) Bradley, D. C.; Chudzynska, H.; Hammond, M. E.; Hursthouse, M. B.; Motevalli, M.; Ruowen, W. *Polyhedron* **1992**, *11*, 375–379.

(17) Bulky aryloxides^{18,19} and silyloxides²⁰ also form monometallic species.

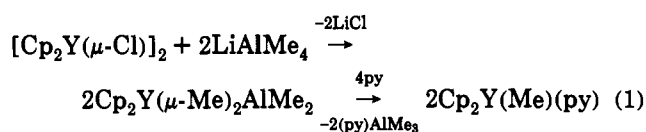
(18) (a) Hitchcock, P. B.; Lappert, M. F.; Smith, R. G. *Inorg. Chim. Acta* **1987**, *139*, 183–184. (b) Stecher, H. A.; Sen, A.; Rheingold, A. L. *Inorg. Chem.* **1988**, *27*, 1130–1132.

(19) Evans, W. J.; Olofson, J. M.; Ziller, J. W. *Inorg. Chem.* **1989**, *28*, 4308–4309.

(20) (a) McGeary, M. J.; Coan, P. S.; Folting, K.; Streib, W. E.; Caulton, K. G. *Inorg. Chem.* **1989**, *28*, 3283–3284. (b) Gradeff, P. S.; Yunlu, K.; Deming, T. J.; Olofson, J. M.; Doedens, R. J.; Evans, W. J. *Inorg. Chem.* **1990**, *29*, 420–424. (c) McGeary, M. J.; Coan, P. S.; Folting, K.; Streib, W. E.; Caulton, K. G. *Inorg. Chem.* **1991**, *30*, 1723–1735.

general formulas $\text{Ln}_5(\text{O}-i\text{-Pr})_{13}\text{O}^{6,7,11}$ and $\text{Ln}_6(\text{O}-i\text{-Pr})_{17}\text{Cl}^{3,10}$ ($\text{Ln} = \text{Y, La, Ce, Nd, Pr}$), respectively, are commonly obtained. When the *tert*-butoxide ligand is used, polymetallic species consisting minimally of trimetallic subunits with the general formula $\text{Ln}_3(\text{OR})_3(\mu\text{-OR})_3(\mu_3\text{-OR})(\mu_3\text{-Z})\text{Z}(\text{L})_2$ ($\text{R} = \text{CMe}_3$; $\text{Z} = \text{OR, O, halide}$; $\text{L} = \text{THF, ROH}$) are isolated.^{4,5,8} The following complexes containing this subunit have been characterized by X-ray crystallography: $\text{Y}_3(\text{OCMe}_3)_8\text{Cl}(\text{THF})_2$,⁴ $[\text{Y}_4(\text{OCMe}_3)_{10}\text{Cl}_2\text{O}]^{2-}$,⁴ $\{\text{Y}_3(\text{OCMe}_3)_7(\text{THF})_2\text{Cl}_2\}[\text{Y}_3(\text{OCMe}_3)_7\text{Cl}][\text{YCl}_2]_2$,⁵ $\text{Y}_3(\text{OCMe}_3)_7\text{Cl}_2(\text{THF})_2$,⁵ $\text{Y}_3(\text{OCMe}_3)_7\text{Br}_2(\text{THF})_2$,⁸ and $\text{La}_3(\text{OCMe}_3)_9(\text{HOCMe}_3)_2$.⁹ Other related *tert*-butoxide compounds have shown NMR spectra characteristic of this subunit.^{4,5,8,9} Further development of yttrium and lanthanide *tert*-butoxide chemistry was expected to generate complexes which were minimally trimetallic. We report here on efforts to make alkylaluminum derivatives of the trimetallic *tert*-butoxide species and the surprising chemistry which ensued.

One of the traditional routes to alkyl and alkylaluminum derivatives of yttrium and lanthanide cyclopentadienyl complexes is the reaction of a reactive metal chloride complex with LiAlMe_4 , followed by cleavage of trimethylaluminum by pyridine (eq 1)



($\text{Cp} = \text{C}_5\text{H}_5$, $\text{py} = \text{C}_5\text{H}_5\text{N}$).²¹ The closest analog of the bis(cyclopentadienyl) chloro complex $[\text{Cp}_2\text{Y}(\mu\text{-Cl})]_2$ in yttrium *tert*-butoxide chemistry is the trimetallic dichloride complex $\text{Y}_3(\text{OCMe}_3)_7\text{Cl}_2(\text{THF})_2$ (1).⁵ The reactions of 1 with AlMe_3 and LiAlMe_4 are described here as well as their implications with respect to the trimetallic chemistry of yttrium *tert*-butoxides, the new opportunities suggested for the synthesis of mixed-metal compounds containing yttrium, and some new structural results involving yttrium halides.

Experimental Section

The syntheses and subsequent manipulations of the compounds described below were conducted with rigorous exclusion of air and water using standard Schlenk, vacuum line, and glovebox techniques.²² ¹H NMR spectra, referenced against the residual protons of THF-*d*₈, toluene-*d*₆, benzene-*d*₆, and cyclohexane-*d*₁₂, were obtained using the following spectrometers: Bruker WM-250, General Electric QE-300, Bruker AC-300, General Electric GN-500, and General Electric Omega-500. Elemental analysis was performed at the Analytische Laboratorien GMBH, Fritz-Pregl-Strasse, 24 D-5270 Gummersbach, Germany. All solvents were freshly distilled under nitrogen from sodium benzophenone. Trimethylaluminum was used as received (Aldrich). LiAlMe_4 was prepared according to literature from the stoichiometric addition of MeLi (Aldrich) to AlMe_3 /hexanes at -78°C .²³ $\text{Y}_3(\text{OCMe}_3)_7\text{Cl}_2(\text{THF})_2$ was prepared from 2.2 equiv of sublimed NaOCMe_3 and YCl_3 by following the literature procedure.⁵

$\text{Y}[(\mu\text{-OCMe}_3)(\mu\text{-Me})\text{AlMe}_2]_2$ (2) and $(\text{Me}_2\text{CO})(\text{THF})\text{Y}[(\mu\text{-OCMe}_3)(\mu\text{-Me})\text{AlMe}_2]_2$ (3). In a glovebox, AlMe_3 (0.50 mL, 5.1 mmol) was slowly added by syringe to a slurry of $\text{Y}_3(\text{OCMe}_3)_7\text{Cl}_2(\text{THF})_2$ (1.70 g, 1.71 mmol) in hexanes (5–8 mL). After the mixture was stirred for 8–12 h, the solvent was removed from the milky solution in vacuo, and the resulting oil was extracted with hexanes. Approximately half of the reaction product was soluble in hexanes. Multiple recrystallizations of the hexanes extract from hexanes at -35°C ultimately gave X-ray-quality crystals which were identified as 2 by X-ray crystallography. The bulk of the hexanes-soluble extract of this reaction was recrystallized at -40°C from toluene to yield 3 (710 mg, 79%). ¹H NMR (500 MHz, 25°C , THF-*d*₈): δ 1.47 (s, 9H, OCMe_3), 1.20 (s, 18H, $\mu\text{-OCMe}_3$), -0.81 (s, 15H, AlMe_2), -0.95

(s, 15H, AlMe_2). ¹³C NMR (500 MHz, 25°C , THF-*d*₈): δ 72.6 (OCMe_3), 70.9 (OCMe_3), 68.0 (THF), 34.6 (OCMe_3), 33.0 (OCMe_3), 26.2 (THF), -4.18 (AlMe_2), -9.35 (AlMe_2). Anal. Calcd for $\text{C}_{22}\text{H}_{53}\text{O}_4\text{Al}_2\text{Y}$: C, 50.38; H, 10.18; Al, 10.28; Y, 16.94. Found: C, 50.41; H, 9.86; Al, 10.40; Y, 16.70.

X-ray Data Collection and Structure Determination and Refinement for $\text{Y}[(\mu\text{-OCMe}_3)(\mu\text{-Me})\text{AlMe}_2]_2$ (2). Under nitrogen, a colorless crystal of approximate dimensions $0.33 \times 0.37 \times 0.37$ mm was immersed in Paratone-D oil.²⁴ The oil-coated crystal was then manipulated in air onto a glass fiber and transferred to the nitrogen stream of a Siemens P3 diffractometer (R3m/V System) which was equipped with a modified LT-2 low-temperature system. Subsequent setup operations (determination of accurate unit cell dimensions and orientation matrix) and collection of low-temperature (173 K) intensity data were carried out using standard techniques similar to those of Churchill.²⁵ Details appear in Table I.

All 2589 data were corrected for absorption and for Lorentz and polarization effects, merged to yield a unique data set, and placed on an approximately absolute scale. Diffraction symmetry indicated a trigonal crystal system with systematic absences for $hh2hl$ where $l = 2n + 1$. The two possible space groups were noncentrosymmetric $P31c$ [C_{3v}^4 ; No. 159] and centrosymmetric $P\bar{3}1c$ [D_{3d}^2 ; No. 163]. The Z value was 2, and the molecule had molecular 3-fold symmetry. The noncentrosymmetric space group was consistent with $Z = 2$ and with the molecular symmetry and was later determined to be correct by successful solution and refinement of the structure.

All crystallographic calculations were carried out using either our locally modified version of the UCLA Crystallographic Computing Package²⁶ or the SHELXTL PLUS program set.²⁷ The analytical scattering factors for neutral atoms were used throughout the analysis;²⁸ both the real ($\Delta f'$) and imaginary ($i\Delta f''$) components of anomalous dispersion²⁸ were included. The quantity minimized during least-squares analysis was $\sum w(|F_o| - |F_c|)^2$ where $w^{-1} = \sigma^2(|F_o|) + 0.0003(|F_o|)^2$.

The structure was solved by direct methods (SHELXTL) and refined by full-matrix least-squares techniques. The molecule was located about a 3-fold rotation axis (yttrium coordinates $1/3, 2/3, z$). Hydrogen atoms were included using a riding model with $d(\text{C-H}) = 0.96 \text{ \AA}$ and $U(\text{iso}) = 0.08 \text{ \AA}^2$. Refinement of positional and thermal parameters led to convergence with $R_F = 9.9\%$, $R_{wF} = 13.4\%$, and $\text{GOF} = 4.79$ for 86 variables refined against those 799 data with $|F_o| > 4.0\sigma(|F_o|)$. A final difference-Fourier map yielded $\rho(\text{max}) = 6.37 \text{ e \AA}^{-3}$ at $(0, 0, z)$. This residual electron density is not chemically or crystallographically consistent with a solvent molecule, anion/cation, etc. (no charge balance is necessary for the structure). Attempts to determine the identity of this atom were inconclusive. The best results were obtained when this atom was refined as an oxygen. The resultant $U(\text{iso})$ was 0.05 \AA^2 , and the discrepancy indices were $R_F = 7.1\%$ and $R_{wF} = 9.7\%$. Since no definitive conclusion as to the composition of this atom could be reached, it was not included in the final refinement of the model.

X-ray Data Collection and Structure Determination and Refinement for $(\text{Me}_2\text{CO})(\text{THF})\text{Y}[(\mu\text{-OCMe}_3)(\mu\text{-Me})\text{AlMe}_2]_2$ (3). Under nitrogen, a colorless crystal of approximate dimensions $0.27 \times 0.33 \times 0.53$ mm was handled as described above for 2.²⁴ Intensity data were collected at 168 K using a θ - 2θ scan technique with $\text{Mo K}\alpha$ radiation under the conditions listed in Table I. All 2294 data were corrected for absorption and for Lorentz and polarization effects and placed on an approximately absolute scale. The diffraction symmetry was *mmm* with systematic absences $0kl$ for $l = 2n + 1$ and $h0l$ for $h = 2n + 1$. The two possible orthorhombic space groups were noncentrosymmetric $Pca2_1$ [C_{2v}^2 ; No. 29] and centrosymmetric $Pbcm$ [D_{2h}^{11} ; No. 57] (standard setting of $Pcam$). It was

(24) While the crystals were mounted in Paratone-D oil, bubbling could be observed which was not attributable to the decomposition of the crystal but to some reaction involving the oil and the mother liquor from the crystals. To investigate the possibility that the oil contained some reactive basic sites, AlMe_3 was syringed onto Paratone-D and vigorously shaken. Substantial bubbling was once again observed, and a subsequent ¹H NMR spectrum of this product on THF-*d*₈ indicated that one of the original peaks of Paratone-D oil was greatly diminished. A resonance associated with unreacted AlMe_3 was also noted.

(25) Churchill, M. R.; Lashewycz, R. A.; Rotella, F. J. *Inorg. Chem.* **1977**, *16*, 265–271.

(26) (a) *UCLA Crystallographic Computing Package*; University of California: Los Angeles, CA, 1981. (b) Strouse, C. Personal communication.

(27) *SHELXTL PLUS*; Siemens Analytical X-ray Instruments, Inc.: Madison, WI, 1990.

(28) *International Tables for X-ray Crystallography*; Kynoch Press: Birmingham, England, 1974; Vol. IV: (a) pp 99–101; (b) pp 149–150.

(21) Holton, J.; Lappert, M. F.; Ballard, D. G. H.; Pearce, R.; Atwood, J. L.; Hunter, W. E. *J. Chem. Soc., Dalton Trans.* **1979**, 54–61.

(22) Evans, W. J.; Chamberlain, L. R.; Ulibarri, T. A.; Ziller, J. W. *J. Am. Chem. Soc.* **1988**, *110*, 6423–6432.

(23) (a) Schlesinger, H. I.; Brown, H. C. *J. Am. Chem. Soc.* **1940**, *62*, 3429–3435. (b) Finholt, A. E.; Bond, A. C., Jr.; Schlesinger, H. I. *J. Am. Chem. Soc.* **1947**, *69*, 1199–1203.

Table I. Experimental X-ray Data for $Y[(\mu\text{-OCMe}_3)(\mu\text{-Me})\text{AlMe}_2]_3$ (2), $(\text{Me}_3\text{CO})(\text{THF})Y[(\mu\text{-OCMe}_3)(\mu\text{-Me})\text{AlMe}_2]_2$ (3), $\text{YCl}_3(\text{DME})_2$ (5), and $[(\text{THF})_3Y(\mu\text{-Cl})_3Y_3(\mu_3\text{-OCMe}_3)(\mu\text{-OCMe}_3)_3(\text{OCMe}_3)_3(\mu_4\text{-O})]$ (6)

	2	3	5	6
formula	$\text{C}_{22}\text{H}_{54}\text{O}_3\text{Al}_3\text{Y}$	$\text{C}_{22}\text{H}_{53}\text{O}_4\text{Al}_2\text{Y}$	$\text{C}_8\text{H}_{20}\text{O}_4\text{Cl}_3\text{Y}$	$\text{C}_{40}\text{H}_{87}\text{O}_{11}\text{Cl}_3\text{Y}_4$
fw	524.5	524.5	375.5	1206.1
temp (K)	173	168	168	173
crystal system	trigonal	orthorhombic	monoclinic	rhombohedral
space group	$P31c [C_{3v}^4; \text{no. 159}]$	$Pca2_1 [C_{2v}^5; \text{No. 29}]$	$P2_1/c [C_{2h}^2; \text{No. 14}]$	$R\bar{3} [C_{3v}^6; \text{No. 148}]$
<i>a</i> (Å)	15.842(2)	14.408(4)	11.343(5)	14.615(3)
<i>b</i> (Å)		17.216(3)	8.855(3)	
<i>c</i> (Å)	7.9994(14)	12.186(2)	15.617(9)	50.993(12)
β (deg)			104.59(4)	
<i>V</i> (Å ³)	1738.6(4)	3022(11)	1518.1(12)	9433(3)
<i>Z</i>	2	4	4	6
<i>D</i> _{calc} (Mg/m ³)	1.002	1.153	1.643	1.274
diffractometer	Siemens P3 (R3m/v System)	Siemens P3 (R3m/v System)	Siemens P3 (R3m/v System)	Siemens P3 (R3m/v System)
radiation (λ (Å))	Mo K α (0.710 730)	Mo K α (0.710 730)	Mo K α (0.710 730)	Mo K α (0.710 730)
monochromator	highly oriented graphite	highly oriented graphite	highly oriented graphite	highly oriented graphite
data collected	$\pm h, +k, +l$	$+h, +k, +l$	$+h, +k, \pm l$	$\pm h, +k, +l$
scan type	θ -2 θ	θ -2 θ	θ -2 θ	θ -2 θ
scan width (deg)	1.20 + K α separation	1.20 + K α separation	1.20 + K α separation	1.20 + K α separation
scan speed (in ω) (deg min ⁻¹)	3.0	3.0	3.0	3.0
2 θ range (deg)	4.0–45.0	4.0–45.0	4.0–45.0	4.0–45.0
μ (Mo K α) (mm ⁻¹)	1.78	2.02	4.40	3.85
abs cor	semiempirical (ψ -scan method)	semiempirical (ψ -scan method)	semiempirical (ψ -scan method)	semiempirical (ψ -scan method)
no. of reflns collected	2589	2294	2284	4385
no. of unique reflns	835	2026	1876	2485
with ($ F_o > 0$)				
no. of reflns with ($ F_o > X\sigma(F_o)$)	799 ($X = 4.0$)	1848 ($X = 3.0$)	1659 ($X = 3.0$)	1344 ($X = 6.0$)
no. of variables	86	262	224	109
<i>R</i> _F (%)	9.9	4.5	3.2	7.8
<i>R</i> _{wF} (%)	13.4	4.4	3.6	10.9
goodness of fit	4.79	1.54	1.06	2.12

later shown by successful refinement of the model that the noncentrosymmetric space group was correct. Details appear in Table I.

All crystallographic calculations were carried out as described above for 2. The structure was solved by direct methods (SHELXTL PLUS) and refined by full-matrix least-squares techniques. Hydrogen atoms were included using a riding model with $d(\text{C-H}) = 0.96$ Å and $U(\text{iso}) = 0.08$ Å². The relative positions of the hydrogen atoms attached to C(15) and C(16) were determined from a difference-Fourier map and then refined as above. Refinement of positional and anisotropic thermal parameters led to convergence with $R_F = 4.5\%$, $R_{wF} = 4.4\%$, and $\text{GOF} = 1.54$ for 262 variables refined against those 1848 data with $|F_o| > 3.0\sigma(|F_o|)$. The absolute structure was determined from the diffraction experiment by refinement of the Rogers η -parameter.²⁹ A final difference-Fourier synthesis yielded $\rho(\text{max}) = 0.53$ e Å⁻³.

$(\text{Me}_3\text{CO})(\text{Cl})(\text{THF})_2Y[(\mu\text{-OCMe}_3)_2\text{AlMe}_2]$ (4). The hexanes-insoluble portion formed in an analogous reaction run as above for 2 and 3 (0.500 g, 0.500 mmol of 1; 0.145 mL, 1.50 mmol of AlMe_3) was extracted with THF, and the small amount of insoluble material was discarded. Removal of solvent by rotary evaporation left a white powder (253 mg). Attempts to crystallize this powder from THF did not yield X-ray-quality crystals, but recrystallization at -35 °C from a concentrated THF solution (2 mL) containing 5–10 drops of DME produced crystals of 4 identified by X-ray diffraction. ¹H NMR (500 MHz, 25 °C, THF-*d*₆): δ 1.48 (s, 18H, OCMe_3), 1.23 (s, 9H, OCMe_3), -0.746 (s, 6H, AlMe_2). ¹³C NMR (500 MHz, 25 °C, THF-*d*₆): δ 72.8 (OCMe_3), 71.6 (OCMe_3), 68.0 (THF), 34.1 (OCMe_3), 32.6 (OCMe_3), 26.2 (THF), -2.694 (AlMe_2).

X-ray Data Collection and Structure Determination and Refinement for $(\text{Me}_3\text{CO})(\text{Cl})(\text{THF})_2Y[(\mu\text{-OCMe}_3)_2\text{AlMe}_2]$ (4). Under nitrogen, crystals of 4 were placed in Paratone-D oil. A crystal was mounted onto a Siemens P3 diffractometer equipped with a modified LT-2 low-temperature system. Since the crystal was of poor quality, a 2 θ data set range of 4.0–45.0° was collected at 173 K and only the atomic connectivity of the compound could be unambiguously determined. 4 crystallized from THF/DME in space group *Pnma* with $a = 19.752(25)$ Å, $b = 12.765(28)$ Å, $c = 11.938(10)$ Å, $V = 3010(8)$ Å³, and $D_{\text{calc}} = 1.09$ Mg/m³ for $Z = 4$. A total of 4337 reflections were collected, and a least-squares refinement of the model based on 1978 observed reflections ($|F_o| > 4.0\sigma(|F_o|)$) converged to a final $R_F = 15.0\%$.

X-ray Data Collection and Structure Determination, and Refinement for $\text{YCl}_3(\text{CH}_3\text{OCH}_2\text{CH}_2\text{OCH}_3)_2$ (5). Recrystallization of a THF-soluble

fraction identical to that used above to obtain 4, using a 3:1 ratio of THF:DME, resulted in crystals of 5 in very low yield. Under nitrogen, a colorless crystal of approximate dimensions 0.30 × 0.40 × 0.40 nm was handled as described above for 2. Intensity data were collected at 168 K using a θ -2 θ scan technique with Mo K α radiation under the conditions given in Table I. All 7579 data were corrected for absorption and for Lorentz and polarization effects and placed on an approximately absolute scale. Any reflection with $I(\text{net}) < 0$ was assigned the value $|F_o| = 0$. The systematic extinctions observed were $0k0$ for $k = 2n + 1$ and $h0l$ for $l = 2n + 1$. The diffraction symmetry was 2/*m*. The centrosymmetric monoclinic space group $P2_1/c [C_{2h}^2; \text{No. 14}]$ was uniquely defined. Details appear in Table I.

All crystallographic calculations were carried out as described above for 2. The structure was solved by direct methods (SHELXTL PLUS) and refined by full-matrix least-squares techniques. Hydrogen atoms were located from a series of difference-Fourier maps and included with isotropic temperature factors. The temperature factors of H(3A) and H(6A) refined to unacceptably low values and were fixed at $U(\text{iso}) = 0.04$ Å². Refinement of positional and thermal parameters led to convergence with $R_F = 3.2\%$, $R_{wF} = 3.6\%$, and $\text{GOF} = 1.06$ for 224 variables refined against those 1659 data with $|F_o| > 3.0\sigma(|F_o|)$. A final difference-Fourier synthesis yielded $\rho(\text{max}) = 0.40$ e Å⁻³.

$\text{YCl}_3(\text{THF})_3Y_3(\text{OCMe}_3)_7\text{O}$ (6). In the glovebox, LiAlMe_4 (0.020 g, 0.20 mmol) was added to $Y_3(\text{OCMe}_3)_7\text{Cl}_2(\text{THF})_2$ (0.20 g, 0.20 mmol) dissolved in toluene (10 mL) in a 25-mL Schlenk flask fitted with a reflux condenser. The mixture was stirred for 30 min, attached to a Schlenk line, and heated at reflux. After 4 h, a white precipitate was present. After 12 h, the solution was cooled to room temperature, and the solvent was removed in vacuo. Extraction with hexanes gave a white powder (154 mg) which displayed a very complicated ¹H NMR spectrum. Crystallization of a toluene solution of this powder at -35 °C for 2 weeks produced crystals which also had multiple peaks in the NMR spectrum. ¹H NMR (300 MHz, 25 °C, THF-*d*₆): δ 1.93, 1.91, 1.89 ($\mu_3\text{-OCMe}_3$), 1.67, 1.61 ($\mu\text{-OCMe}_3$), 1.34, 1.36, 1.37 (OCMe_3). X-ray crystallographic analysis of one crystal identified $\text{YCl}_3(\text{THF})_3Y_3(\text{OR})_7\text{O}$ (6) as a component of the mixture.

X-ray Data Collection and Structure Determination and Refinement for $\text{YCl}_3(\text{THF})_3Y_3(\text{OCMe}_3)_7\text{O}$ (6). Under nitrogen, a colorless crystal of approximate dimensions 0.17 × 0.25 × 0.37 mm was handled as described above for 2. Intensity data were collected at 173 K. Details appear in Table I. All 4385 data were corrected for absorption and for

(29) Rogers, D. *Acta Crystallogr., Sect. A* 1981, *A37*, 734–741.

Lorentz and polarization effects, merged to yield a unique data set, and placed on an approximately absolute scale. Diffraction symmetry indicated a rhombohedral crystal system with systematic absences for hkl where $-h + k + l = 3n + 1$. The two possible space groups were noncentrosymmetric $R\bar{3}$ and centrosymmetric $R\bar{3}$. The latter was chosen and determined to be correct by successful solution and refinement of the structure. All crystallographic calculations were carried out as described above for **2**. The quantity minimized during least-squares analysis was $\sum w(|F_o| - |F_c|)^2$ where $w^{-1} = \sigma^2(|F_o|) + 0.0010(|F_o|)^2$.

The structure was solved by direct methods (SHELXTL PLUS) and refined by full-matrix least-squares techniques. The molecule was located on a site of 3-fold symmetry ($2/3, 1/3, z$). Hydrogen atoms were included using a riding model with $d(\text{C-H}) = 0.96 \text{ \AA}$ and $U(\text{iso}) = 0.08 \text{ \AA}^2$. Refinement of positional and thermal parameters led to convergence with $R_p = 7.8\%$, $R_{wF} = 10.9\%$, and $\text{GOF} = 2.12$ for 109 variables refined against those 4536 data with $|F_o| > 6.0\sigma(|F_o|)$. A final difference-Fourier map was devoid of significant features; $\rho(\text{max}) = 2.13 \text{ e \AA}^{-3}$.

Results

The $\text{Y}_3(\text{OCMe}_3)_7\text{Cl}_2(\text{THF})_2/\text{AlMe}_3$ System. Synthesis. $\text{Y}_3(\text{OCMe}_3)_7\text{Cl}_2(\text{THF})_2$ (**1**) was treated with 1 equiv of trimethylaluminum in hexanes to determine if a simple AlMe_3 adduct involving a $\text{Y}(\mu\text{-Cl})(\mu\text{-Me})\text{AlMe}_2$ or $\text{Y}(\mu\text{-OCMe}_3)(\mu\text{-Me})\text{AlMe}_2$ unit would form. A reaction occurred at room temperature, and extraction of the resulting solids with hexanes, toluene, and THF indicated that a mixture of products was present. One major component of the reaction mixture was hexanes soluble, and the other was THF soluble. The $^1\text{H NMR}$ spectrum of the hexanes-soluble material (vide infra) did not have the characteristic six-line pattern found in $\text{THF-}d_8$ for trimetallic species such as **1**.^{4,5} Instead, the $\text{THF-}d_8$ spectrum displayed four sharp resonances: two in the *tert*-butoxide region (δ 1.47 and 1.20) and two in the methylaluminum region (δ -0.81 and -0.95). These data indicated that the trimetallic structure was no longer intact.

Reactions between $\text{Y}_3(\text{OCMe}_3)_7\text{Cl}_2(\text{THF})_2$ and AlMe_3 using various stoichiometries, including 1:2, 1:3, and 1:10, gave products with the same $^1\text{H NMR}$ spectra, and the ratio of 1:3 gave the highest yield. Reactions involving a larger excess of AlMe_3 led only to an increase in the amount of AlMe_3 present in the hexanes-soluble fraction. When the 1:3 reaction was carried out in toluene, the yields were lower and additional side products were observed. When **1** was treated with AlMe_3 in THF, the starting material **1** was recovered intact, presumably due to the formation of $\text{AlMe}_3(\text{THF})$.³⁰

Product Identification. Since the $^1\text{H NMR}$ spectrum of the hexanes-soluble material was not structurally informative, characterization by X-ray crystallography was attempted. After multiple recrystallizations from hexanes, single crystals were obtained and structurally identified as the monometallic yttrium complex $\text{Y}[(\mu\text{-OCMe}_3)(\mu\text{-Me})\text{AlMe}_2]_3$ (**2**) (Figure 1). Crystallization of the same material from toluene also gave X-ray-quality crystals, but X-ray diffraction revealed that this was a different monoyttrium product, $(\text{Me}_3\text{CO})(\text{THF})\text{Y}[(\mu\text{-OCMe}_3)(\mu\text{-Me})\text{AlMe}_2]_2$ (**3**) (Figure 2), which varied from the structure of **2** by the absence of an AlMe_3 unit and the addition of a THF ligand. The structural data confirmed the conclusion drawn from the NMR data that the trimetallic framework of the starting material had been completely disrupted in this reaction. Furthermore, both **2** and **3** were halide free, a result which was quite surprising since retention of chloride in yttrium *tert*-butoxide chemistry has always been observed in the past, e.g. in the complexes $\text{Y}_3(\text{OCMe}_3)_8\text{Cl}(\text{THF})_2$,⁴ $[\text{Y}_4(\text{OCMe}_3)_{10}\text{Cl}_2\text{O}]^{2-}$,⁴ $\text{Y}_3(\text{OCMe}_3)_7\text{Cl}_2(\text{THF})_2$,⁵ $\text{Y}_{14}(\text{OCMe}_3)_{28}\text{Cl}_{10}\text{O}_2(\text{THF})_4$,⁵ $[\text{Y}_2(\text{OCMe}_3)_4\text{Cl}(\text{THF})_4]^+$,³¹ and $[\text{Y}(\text{OCMe}_3)\text{Cl}(\text{THF})_5]^+$.³¹

Attempts to locate chloride-containing products focused on the THF-soluble component of the reaction. The $^1\text{H NMR}$

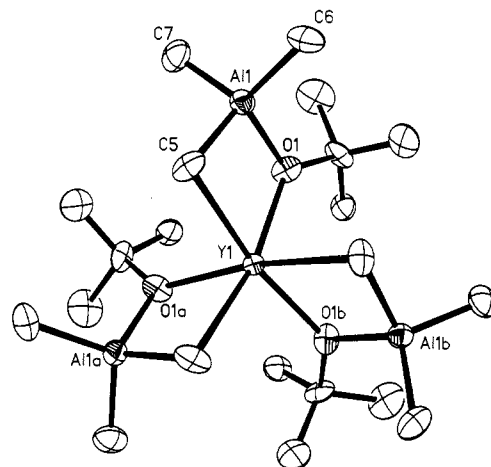


Figure 1. ORTEP diagram of $\text{Y}[(\mu\text{-OCMe}_3)(\mu\text{-Me})\text{AlMe}_2]_3$ (**2**) with probability ellipsoids drawn at the 50% level.

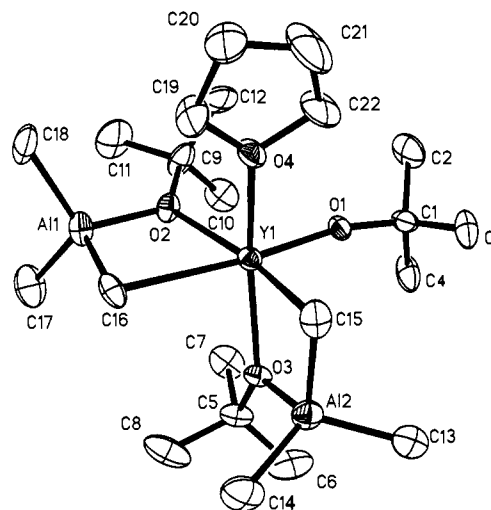


Figure 2. ORTEP diagram of $(\text{Me}_3\text{CO})(\text{THF})\text{Y}[(\mu\text{-OCMe}_3)(\mu\text{-Me})\text{AlMe}_2]_2$ (**3**) with probability ellipsoids drawn at the 50% level.

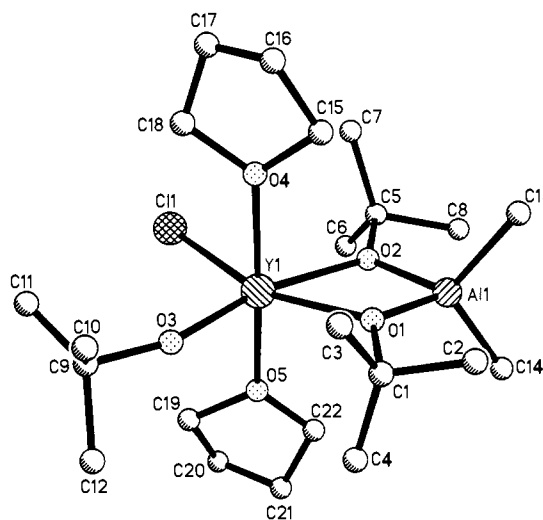


Figure 3. Ball and stick diagram of $(\text{Me}_3\text{CO})\text{Cl}(\text{THF})_2\text{Y}[(\mu\text{-OCMe}_3)_2\text{AlMe}_2]$ (**4**).

spectrum of this fraction also indicated that a mixture of products was present. However, crystallization in the presence of a small amount of dimethoxyethane (DME) gave single crystals of $(\text{Me}_3\text{CO})(\text{Cl})(\text{THF})_2\text{Y}[(\mu\text{-OCMe}_3)_2\text{AlMe}_2]$ (**4**) (Figure 3). This complex is similar to **2** and **3** in that it is a monoyttrium complex with a bridging alkoxide-aluminum ligand. However, in this

(30) Mole, T.; Jeffery, E. A. *Organoaluminum Compounds*; Elsevier: New York, 1972; pp 106-110.

(31) Evans, W. J.; Olofson, J. M.; Ziller, J. W. *J. Am. Chem. Soc.* **1990**, *112*, 2308-2314.

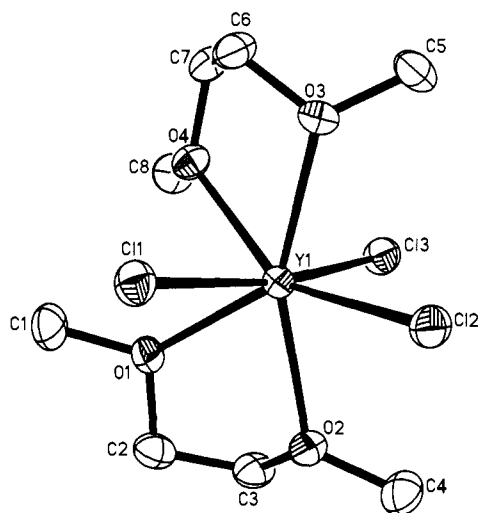


Figure 4. ORTEP diagram of $\text{YCl}_3(\text{DME})_2$ (**5**) with probability ellipsoids drawn at the 50% level.

case, the aluminum-containing bridge is a $(\mu\text{-OR})_2\text{AlMe}_2$ unit instead of a $(\mu\text{-OR})(\mu\text{-Me})\text{AlMe}_2$ moiety. Obviously, some ligand rearrangement occurred in the course of the reaction, and it occurred to form the alkoxide bridges preferentially. This is consistent with structural data on mixed alkyl-alkoxide-aluminum compounds, which have alkoxides in the bridging positions.^{32,33} Product **4** does indeed contain a chloride ligand, as anticipated. The NMR spectrum of crystals of **4** shows that it comprises a large part of the THF component of this reaction.

In attempts to identify other components of the THF-soluble product mixture, crystallizations with different ratios of THF and DME were examined. With a 3:1 mixture of THF and DME, a mixture of crystals was obtained. The ^1H NMR spectrum of the mother liquor indicated that **4** was the predominant product. When the crystals were placed under Paratone-D oil for X-ray diffraction studies, some appeared to decompose more readily than others. One of the more stable crystals was crystallographically identified as $\text{YCl}_3(\text{DME})_2$ (**5**) (Figure 4). Complex **5** is the first monometallic yttrium trihalide characterized by X-ray crystallography.³⁴ The overall reaction is shown in Scheme I.

X-ray Diffraction Studies on 2-4. As shown in Figures 1-3, complexes **2-4** each contain a single yttrium atom in a six-coordinate distorted octahedral environment. Although a coordination number of 8 is more typical for yttrium and lanthanide organometallic complexes,³⁵ six-coordination has been found exclusively in the yttrium and lanthanide *tert*-butoxide structures reported to date.^{4,5,8,31,36} The overall structure of **2-4** resembles that of the homometallic homoleptic aluminum complex $\text{Al}[(\mu\text{-}i\text{-PrO})_2\text{Al}(\text{O-}i\text{-Pr})_2]_3$.³⁷

A detailed comparison of bond distances and angles can be made between complexes **2** and **3** (Tables II and III), but the

(32) (a) Haaland, A.; Stokkeland, O. *J. Organomet. Chem.* **1975**, *94*, 345-352. (b) Kai, Y.; Yasuoka, N.; Kasai, N.; Kakudo, M. *J. Organomet. Chem.* **1971**, *32*, 165-179.

(33) See also: Mason, R.; Mingos, D. M. P. *J. Organomet. Chem.* **1973**, *50*, 53-61.

(34) For a subsequent example, see: Evans, W. J.; Shreeve, J. L.; Ziller, J. W. *Inorg. Chem.*, in press.

(35) (a) Marks, T. J.; Ernst, R. D. In *Comprehensive Organometallic Chemistry*; Wilkinson, G., Stone, F. G. A., Abel, E. W., Eds.; Pergamon Press: New York, 1982; Chapter 21. (b) Forsberg, J. H.; Moeller, T. In *Gmelin Handbook of Inorganic Chemistry*, 8th ed.; Moeller, T., Krueker, U., Schleitzer-Rust, E., Eds.; Springer-Verlag: Berlin, 1983; Part D6, pp 137-282. (c) Schumann, H.; Genthe, W. In *Handbook on the Physics and Chemistry of Rare Earths*; Gschneidner, K. A., Jr., Eyring, L., Eds.; Elsevier: Amsterdam, 1985; Vol 7, Chapter 53 and references therein. (d) Evans, W. J.; Foster, S. E. *J. Organomet. Chem.* **1992**, *433*, 79-94.

(36) Six-coordination is also found in isopropoxide complexes,^{3,6,7,10} but $[\text{Y}(\text{OC}_2\text{H}_4\text{OMe})_3]_{10}$ contains seven-coordinate yttrium.¹²

(37) Foltling, K.; Streib, W. E.; Caulton, K. G.; Poncelet, O.; Hubert-Pfalzgraf, L. G. *Polyhedron* **1991**, *10*, 1639-1646. Turova, N. Ya.; Kozunov, V. A.; Yanovskii, A. I.; Bokii, N. G.; Struchkov, Yu. T.; Tarnopol'skii, B. L. *J. Inorg. Nucl. Chem.* **1979**, *41*, 511.

Scheme I. Reaction of $\text{Y}_3(\text{OCMe}_3)_7\text{Cl}_2(\text{THF})_2$ (**1**), with AlMe_3

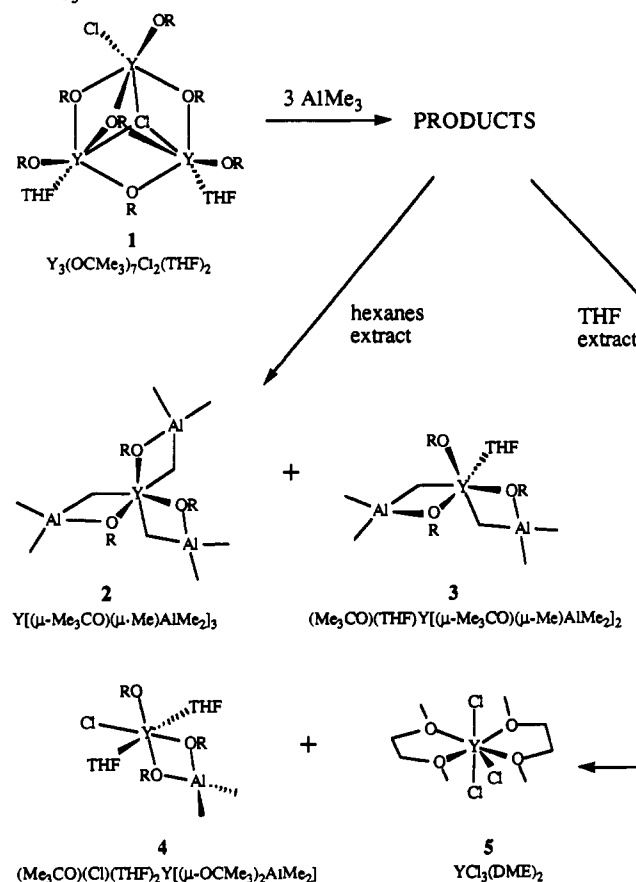


Table II. Bond Distances (Å) for $\text{Y}[(\mu\text{-OCMe}_3)(\mu\text{-Me})\text{AlMe}_2]_3$ (**2**) and $(\text{Me}_3\text{CO})(\text{THF})\text{Y}[(\mu\text{-OCMe}_3)(\mu\text{-Me})\text{AlMe}_2]_2$ (**3**)

	2	3
Y(1)-O(1)	2.209(14)	Y(1)-O(1) 2.005(4) Y(1)-O(2) 2.252(5) Y(1)-O(3) 2.256(6) Y(1)-O(4) 2.388(7)
Y(1)-C(5)	2.688(28)	Y(1)-C(15) 2.668(10) Y(1)-C(16) 2.735(6)
Al(1)-O(1)	1.864(20)	Al(1)-O(2) 1.841(5) Al(2)-O(3) 1.841(6)
Al(1)-C(5)	2.095(21)	Al(1)-C(16) 2.053(7) Al(2)-C(15) 2.045(11)
Al(1)-C(6)	1.946(23)	Al(1)-C(17) 1.973(11)
Al(1)-C(7)	2.014(33)	Al(1)-C(18) 1.969(11) Al(2)-C(13) 1.966(10) Al(2)-C(14) 1.983(10)
Y(1)···Al(1)	3.195(7)	Y(1)···Al(1) 3.244(3) Y(1)···Al(2) 3.200(3)

quality of the data obtained on **4** allows only a general description of the atomic connectivity. The angles around yttrium in **2** and **3** (Table III) show that the distortion from pure octahedral is similar in both complexes and that sterically a terminal alkoxide and a THF molecule are similar to a chelating $[(\mu\text{-OCMe}_3)(\mu\text{-Me})\text{AlMe}_2]$ group. Table III also shows the similarity between the angles around the aluminum atoms in **2** and **3**, both of which have distorted tetrahedral geometries. The Y-C(Me)-Al angles of **2** ($82.8(9)^\circ$) and **3** ($84.4(3)$ and $84.0(2)^\circ$) are also similar and are comparable to the analogous angles of $81.5(7)$ and $80.1(7)^\circ$ in $(\text{C}_5\text{H}_5)_2\text{Y}(\mu\text{-Me})_2\text{AlMe}_2$ (**7**).³⁸ The Y-O-Al angles in **2** and **3** are substantially larger than the Y-C-Al angles, which makes the Y-C-Al-O core an irregular rhombohedron.

Table III. Bond Angles (deg) for $Y[(\mu\text{-OCMe}_3)(\mu\text{-Me})\text{AlMe}_2]_3$ (**2**) and $(\text{Me}_3\text{CO})(\text{THF})Y[\mu\text{-OCMe}_3](\mu\text{-Me})\text{AlMe}_2]_2$ (**3**)

2		3	
Trans Ligand-Y-Trans Ligand Angles			
C(5)-Y(1)-O(1B)	159.8(7)	O(1)-Y(1)-C(16)	174.6(2)
		O(2)-Y(1)-C(15)	158.5(2)
		O(3)-Y(1)-O(4)	151.1(2)
Cis Ligand-Y-Cis Ligand Angles			
O(1)-Y(1)-C(5)	75.2(6)	O(1)-Y(1)-C(15)	95.4(2)
O(1A)-Y(1)-C(5)	88.8(7)	O(2)-Y(1)-C(16)	72.3(2)
O(1)-Y(1)-O(1A)	108.2(4)	O(3)-Y(1)-C(15)	73.6(3)
		O(3)-Y(1)-C(16)	85.1(3)
		O(4)-Y(1)-C(15)	78.6(3)
		O(4)-Y(1)-C(16)	86.2(3)
		O(1)-Y(1)-O(2)	103.3(2)
		O(1)-Y(1)-O(3)	99.6(2)
		O(1)-Y(1)-O(4)	90.8(2)
		O(2)-Y(1)-O(3)	112.9(2)
		O(2)-Y(1)-O(4)	90.5(2)
C(5)-Y(1)-C(5A)	85.0(7)	C(15)-Y(1)-C(16)	88.3(3)
Angles Around Aluminum			
O(1)-Al(1)-C(5)	98.9(9)	O(3)-Al(2)-C(15)	99.5(4)
O(1)-Al(1)-C(6)	113.8(11)	O(2)-Al(1)-C(16)	99.2(3)
O(1)-Al(1)-C(7)	112.1(10)	O(2)-Al(1)-C(17)	110.8(4)
		O(2)-Al(1)-C(18)	113.9(4)
		O(3)-Al(2)-C(13)	113.3(4)
		O(3)-Al(2)-C(14)	109.7(4)
C(5)-Al(1)-C(6)	106.7(10)	C(16)-Al(1)-C(17)	109.1(5)
C(5)-Al(1)-C(7)	107.7(11)	C(16)-Al(1)-C(18)	108.7(4)
C(6)-Al(1)-C(7)	115.8(12)	C(13)-Al(2)-C(15)	105.4(4)
		C(14)-Al(2)-C(15)	109.0(4)
		C(17)-Al(1)-C(18)	113.9(4)
		C(13)-Al(2)-C(14)	118.1(4)
Central Core Angles			
Y(1)-O(1)-Al(1)	103.1(7)	Y(1)-O(2)-Al(1)	104.4(2)
		Y(1)-O(2)-Al(2)	102.2(3)
Y(1)-C(5)-Al(1)	82.8(9)	Y(1)-C(15)-Al(2)	84.4(3)
		Y(1)-C(16)-Al(1)	84.0(2)

The Y(1)-O($\mu\text{-OCMe}_3$) distances in **2** (2.209(14) Å) and **3** (2.252(5) and 2.256(6) Å) are similar, and they overlap with the low end of the 2.19(2)-2.358(10)-Å range found for bridging *tert*-butoxide ligands in other yttrium complexes.^{4,5,31} The 2.005(4)-Å Y(1)-O(1)(OCMe₃) distance in **3** is typical of terminal yttrium *tert*-butoxides (1.97(2)-2.09(3) Å), and the Y(1)-O(4)(THF) distance, 2.388(7) Å, is typical for Y-O(THF), 2.36(2)-2.45(2) Å. The Y(1)-O(1)-C(1) angle for the terminal *tert*-butoxide ligand is 168.4(5)°.

The Y-C($\mu\text{-Me}$) distances [2, Y(1)-C(5) = 2.688(28) Å; 3, Y(1)-C(15) = 2.688(10), Y(1)-C(16) = 2.735(6) Å] are significantly longer than the 2.576-2.60-Å Y-C($\mu\text{-Me}$) distances in **7**.³⁸ These are the first available data on Y-C(methyl) distances in a complex containing alkoxide coligands instead of cyclopentadienyl groups. In comparison, the M-C($\mu\text{-Me}$) distances in alkyl-alkoxide-aluminum complexes are only 0.10-0.15 Å larger than the M-O($\mu\text{-OR}$) distances in [Me₂Al($\mu\text{-OCMe}_3$)]₂.^{32a}

Neutral yttrium *tert*-butoxide complexes crystallographically characterized in the past were exclusively polymetallic, and little could be said about ligand position preferences in the six-coordinate environment of the metal. Complexes **2-4** present the first opportunity to look at ligand site preferences in octahedral monometallic yttrium *tert*-butoxide complexes. In **2**, the three chelating ($\mu\text{-OCMe}_3$)($\mu\text{-Me}$)AlMe₂ groups are arranged such that a carbon atom is always trans to an oxygen atom instead of another carbon. This places the three *tert*-butoxide groups in a facial relationship with respect to each other. Interestingly, a facial arrangement is also observed in (Ph₃SiO)₃Ln(THF)₃ (Ln

= La, Ce, Pr, Y),^{19,20} Y(OC₆H₃Me₂-2,6)₃(THF)₃,¹⁸ Y[OCMe-(CF₃)₂]₃(THF)₃,¹⁶ and Y[OC(CMe₃)₂CH₂PMe₂]₃.¹⁴

The carbon atoms in **3** are similarly oriented trans to oxygen. With the ligand set in this complex, two oxygen donor atoms must be trans to each other, and the arrangement found in **3** places the THF trans to a bridging alkoxide rather than to the terminal alkoxide. Again the three *tert*-butoxide groups occupy facial sites.

With the donor atom set in complex **4**, five oxygens and one chloride, there must be two trans oxygen arrangements. In this case, THF is trans to another THF instead of to an alkoxide and the three *tert*-butoxide groups are meridional. Although there are too few examples here to draw firm conclusions about ligand preferences or even whether the preferences are sterically or electronically controlled, further development of this new class of complexes should provide this information.

The hydrogen atoms of the bridging methyl ligands in **3** were located and refined. The geometry around the bridging carbon atoms is clearly not tetrahedral. The shortest Y...H($\mu\text{-Me}$) distance in **3** is 2.57 Å for Y(1)-H(15B). This is comparable to the 2.54-Å Y-H distance in [Cp₂Y($\mu\text{-Me}$)]₂ (**8**)²¹ and the 2.59(8)-Å Yb-H distance in (C₃Me₅)₂Yb($\mu\text{-Me}$)Be(C₃Me₅) (**9**).³⁹ The metal-carbon distances associated with these short metal-hydrogen distances are not so similar in these three complexes however: **3**, 2.668(10) Å; **8**, 2.537(9), 2.553(10) Å; **9**, 2.766(4) Å.

NMR Studies on 2-4. The ¹H NMR spectrum of crystals of **4** in THF matches the solid-state structure in that there are two resonances in the *tert*-butoxide region in a ratio of 2:1 (δ 1.48 and 1.23), one resonance in the methylaluminum region (δ -0.75), and the appropriate resonances for coordinated THF. The chemical shifts of the alkoxide resonances are consistent with the pattern previously observed for yttrium *tert*-butoxide complexes in which terminal *tert*-butoxides are found at higher field than the bridging ligands.^{4,5}

Analysis of the ¹H NMR spectrum of the hexanes-soluble material was less straightforward. Crystals of **2** and of **3** as well as the bulk powders obtained by precipitating the hexanes-soluble material from hexanes and from toluene (the solvents used to obtain crystals of **2** and **3**, respectively) *all* display the same four resonances in THF. Three of these resonances, δ 1.47, 1.20, and -0.81, are similar to the resonances for **4**. The fourth resonance at δ -0.95 is near the δ -0.91 resonance of AlMe₃ in THF and grows when AlMe₃ is added to the sample. The resonances at δ 1.20 and -0.95 also match the spectrum of the product formed by reacting 1 equiv of *tert*-butyl alcohol with AlMe₃. These results suggested that the hexanes-soluble material was a mixture of complexes which are apparently nonrigid in solution.

However, the solid-state ⁸⁹Y NMR spectrum⁸ of 1.5 g of the bulk sample showed that there was one predominant yttrium-containing component in this mixture, and complete elemental analysis of the bulk material was consistent with the composition of **3**. At least 10 different crystals obtained from a variety of reactions and grown from toluene were examined by X-ray diffraction, and each one had a unit cell identical to **3**. Hence, it must be concluded that **2** is a very minor component of the hexanes-soluble material, and it was fortunate that **2** was isolated by crystallization from hexanes.

Variable-temperature ¹H NMR studies of the hexanes-soluble material were examined in both THF and toluene but provided no additional definitive structural information. In toluene, four resonances are again observed, but two are broad [δ (width at half height, Hz)]: 1.48 (3), 1.34 (0.2), -0.28 (3), -0.46 (0.4). Both broad signals appear to split into two signals at 0 °C. At -20 °C, the sharp signal at δ -0.28 has split and the δ -0.46 signal has lost the splitting observed at 0 °C. At -30 °C, five sharp

(38) (a) Scollary, G. R. *Aust. J. Chem.* **1978**, *31*, 411-414. (b) Holton, J.; Lappert, M. F.; Ballard, G. H.; Pearce, R.; Atwood, J. L.; Hunter, W. E. *J. Chem. Soc., Dalton Trans.* **1979**, 54-61.

(39) Burns, C. J.; Andersen, R. A. *J. Am. Chem. Soc.* **1987**, *109*, 5853-5855.

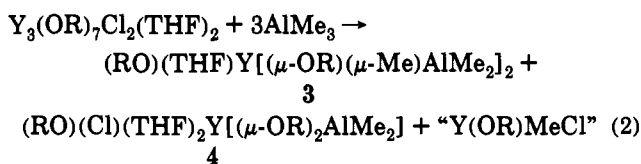
Table IV. Bond Distances (Å) for $YCl_3(DME)_2$ (**5**) and $YCl_3(THF)_3Y_3(OR)_7O$ (**6**)

5		6	
Y(1)–Cl(1)	2.599(2)	Y(1)–Cl(1)	2.751(5)
Y(1)–Cl(2)	2.603(2)	Y(2)–Cl(1)	2.778(5)
Y(1)–Cl(3)	2.597(2)		
Y(1)–O(1)	2.419(4)	Y(1)–O(1)	2.062(12)
Y(1)–O(2)	2.427(3)	Y(1)–O(2)	2.388(12)
Y(1)–O(3)	2.379(3)	Y(1)–O(3)	2.279(18)
Y(1)–O(4)	2.457(3)	Y(1)–O(3A)	2.271(6)
		Y(1)–O(5)	2.304(13)
		Y(2)–O(4)	2.409(17)
		Y(2)–O(5)	2.059(23)
		Y(1)···Y(2)	3.816(4)
		Y(1)···Y(1A)	3.387(3)

signals are observed in the *tert*-butoxide region and two in the methylaluminum region. At -80°C , a different set of five sharp signals is observed in the *tert*-butoxide region and four major and three minor signals are seen in the methylaluminum region. Two distinct sets of THF resonances are also observed at this temperature. At higher temperatures (80°C), the broad peaks sharpen and dominate the spectrum. The sharp peaks at room temperature appear to diminish at higher temperatures. Variable-temperature studies in THF showed no change upon raising the temperature. Upon lowering of the temperature to -40°C , the peak at δ 0.91 is unaffected and the other three resonances become complex multiplets which have substantially decreased in size. The solution behavior of the hexanes-soluble material is obviously complex.

X-ray Diffraction Study of 5. $YCl_3(DME)_2$ (**5**) has a distorted pentagonal bipyramidal structure with chloride ligands in the axial positions (Figure 4). Although this is the first X-ray crystal structure of a simple monomeric yttrium trihalide³⁴ (the closest structurally characterized yttrium analog is the polymeric triethylene glycol (TEG) complex $[YCl_3(TEG)(18\text{-crown-6})]_n$ ⁴⁰), an isostructural gadolinium complex has been reported.⁴¹ In addition, $SmCl_3(DME)(THF)_2$ ⁴² and $LnCl_3(THF)_4$ ($Ln = \text{Eu},^{43} \text{Nd}^{44}$) have similar pentagonal bipyramidal structures with axial chloride ligands. The $169.1(1)^\circ$ Cl(1)–Y(1)–Cl(3) angle in **5** is comparable to the (axial chloride)–metal–(axial chloride) angles in the other pentagonal bipyramidal complexes as are the Y–Cl distances (Table IV), when the differences in metallic radii are taken into account.⁴⁵ The Y–Cl distances in **5** are also equivalent to the 2.595(3)–2.622(2)-Å Y–Cl distances found in the yttrium–TEG complex listed above.⁴⁰ The Y(1)–O(DME) distances in **5** are similarly equivalent to the 2.435(5)-Å Y–O(TEG) distance in that complex.

Synthetic Variations. The reaction describing the two main products found in this system, **3** and **4**, is given in eq 2. The



"Y(OR)MeCl" needed to balance this equation was not isolated and is not likely to exist in that simple form. Since the products

(40) Rogers, R. D.; Voss, E. J.; Etzenhouser, R. D. *Inorg. Chem.* **1988**, *27*, 533–542.

(41) Gecheng, W.; Hanrong, G.; Zhongsheng, J.; Qi, S. *Jiegou Huaxue* **1989**, *8*, 61.

(42) Zhongsheng, J.; Guojun, N.; Ninghai, H.; Wenqi, C. *Yingyong Huaxue* **1989**, *6*, 68.

(43) Lin, S.-H.; Dong, Z.-C.; Huang, J.-S.; Zhang, Q.-E.; Lu, J.-X. *Acta Crystallogr.* **1991**, *C47*, 426–427.

(44) Wenqi, C.; Zhongsheng, J.; Yan, X.; Yuguo, F.; Guandgi, Y. *Inorg. Chim. Acta* **1987**, *130*, 125–129.

(45) Shannon, R. D. *Acta Crystallogr., Sect. A* **1976**, *A32*, 751–767.

Table V. Bond Angles (deg) for $YCl_3(DME)_2$ (**5**) and $YCl_3(THF)_3Y_3(OR)_7O$ (**6**)

5		6	
Cl(1)–Y(1)–Cl(2)	91.2(1)	Cl(1)–Y(2)–Cl(1A)	115.0(1)
Cl(1)–Y(1)–Cl(3)	169.1(1)		
Cl(2)–Y(1)–Cl(3)	97.1(1)		
Cl(1)–Y(1)–O(1)	79.2(1)	Cl(1)–Y(1)–O(1)	100.2(4)
Cl(1)–Y(1)–O(2)	160.9(1)	Cl(1)–Y(1)–O(2)	140.8(4)
Cl(1)–Y(1)–O(3)	85.0(1)	Cl(1)–Y(1)–O(3)	93.2(4)
Cl(1)–Y(1)–O(4)	90.4(1)	Cl(1)–Y(1)–O(3A)	97.5(4)
		Cl(1)–Y(1)–O(5)	73.9(5)
Cl(2)–Y(1)–O(1)	140.7(1)	Cl(1)–Y(2)–O(2)	179.4(15)
Cl(2)–Y(1)–O(2)	80.2(1)	Cl(1)–Y(2)–O(4)	73.6(3)
Cl(2)–Y(1)–O(3)	79.8(1)	Cl(1)–Y(2)–O(5)	76.9(1)
Cl(2)–Y(1)–O(4)	147.0(1)	Cl(1A)–Y(2)–O(4)	152.8(4)
		Cl(1B)–Y(2)–O(4)	80.2(4)
		Cl(1A)–Y(2)–O(5)	76.9(1)
Cl(3)–Y(1)–O(1)	98.4(1)	Y(1)–Cl(1)–Y(2)	87.3(2)
Cl(3)–Y(1)–O(2)	81.5(1)	Y(1)–O(2)–Y(1A)	90.3(6)
Cl(3)–Y(1)–O(3)	89.6(1)	Y(1)–O(3)–Y(1A)	96.2(6)
Cl(3)–Y(1)–O(4)	78.8(1)	Y(1)–O(5)–Y(1A)	94.6(7)
		Y(1)–O(5)–Y(2)	121.9(5)
O(1)–Y(1)–O(2)	66.8(1)	O(1)–Y(1)–O(2)	119.0(6)
O(1)–Y(1)–O(3)	136.1(1)	O(1)–Y(1)–O(3)	106.4(6)
O(1)–Y(1)–O(4)	71.08(1)	O(1)–Y(1)–O(3A)	105.6(7)
O(2)–Y(1)–O(3)	156.8(1)	O(1)–Y(1)–O(3)	74.9(4)
O(2)–Y(1)–O(4)	130.5(1)	O(1)–Y(1)–O(5)	174.1(6)
O(3)–Y(1)–O(4)	67.5(1)	O(1)–Y(1)–O(5)	74.9(3)
		O(2)–Y(1)–O(5)	67.0(6)
		O(3)–Y(1)–O(3A)	143.8(4)
		O(4)–Y(2)–O(4A)	83.1(5)
		O(4)–Y(2)–O(5)	130.0(4)
		O(5)–Y(2)–O(4A)	130.0(4)

of this reaction were not closely related in structure to trimetallic **1**, it seemed likely that other *tert*-butoxide complexes of yttrium could be used as precursors. Indeed, the reaction of $Y_3(OCMe_3)_8Cl(THF)_2$ ⁴ with $AlMe_3$ under the same conditions gave a powder with a ^1H NMR spectrum identical to that of the $Y_3(OCMe_3)_7Cl_2(THF)_2$ reaction product. Apparently, the trimetallic structure of this species also is destroyed by the trimethylaluminum.

Attempts to prepare **2–4** directly from $YCl_3(THF)_3$, $NaOCMe_3$, and $AlMe_3$ were unsuccessful. Combining $YCl_3(THF)_3$ with $AlMe_3$ in toluene gave an insoluble product which did not react with $NaOCMe_3$. Addition of $NaOCMe_3$ to $YCl_3(THF)_3$ to form **1** in situ, followed by addition of $AlMe_3$, gave a more complicated reaction mixture than the synthesis from **1** directly.

Both $AlEt_3$ and $Al(n\text{-Bu})_3$ react with **1** to form products which by NMR are no longer trimetallic. However, in neither case has it been possible to obtain the X-ray crystallographic data needed to unequivocally identify the products. Interestingly, trimethylgallium does not react with **1** even in toluene at reflux temperatures.

The $Y_3(OR)_7Cl_2(THF)_2/LiAlMe_4$ Reaction. Synthesis. The reaction of $LiAlMe_4$ with **1** in hexanes at room temperature for 12 h gave a crude product which possessed a more complex ^1H NMR spectrum than that of the starting material. However, only unchanged **1** was recovered from this system. New products were obtainable, however, by heating **1** and $LiAlMe_4$ in toluene at reflux. The bulk of this reaction mixture was hexanes soluble and displayed a complicated ^1H NMR spectrum indicative of a mixture of products. One component of this mixture was isolated by crystallization and identified by X-ray crystallography as $YCl_3(THF)_3Y_3(OR)_7O$ (**6**) (Figure 5). Even these crystals appeared to be a mixture on the basis of their ^1H NMR spectrum, since multiple resonances were observed in the regions for terminal $OCMe_3$, $\mu\text{-OCMe}_3$, and $\mu_3\text{-OCMe}_3$ ligands attached to yttrium. The thermolysis of **1** in toluene at reflux was independently examined to ensure that $LiAlMe_4$ was necessary for the reaction.

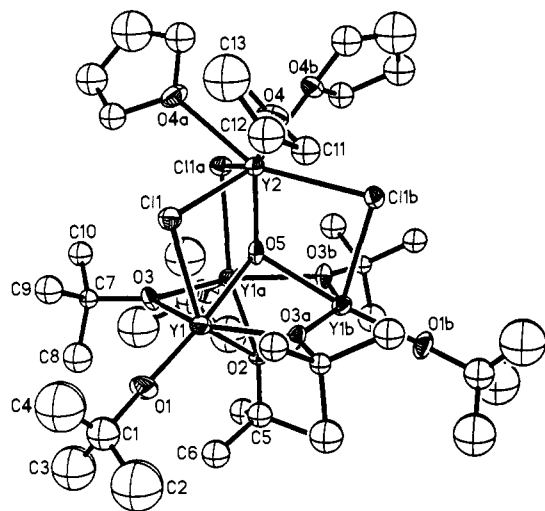


Figure 5. ORTEP diagram of $\text{YCl}_3(\text{THF})_3\text{Y}_3(\text{OR})_7\text{O}$ (**6**) with probability ellipsoids drawn at the 50% level.

The thermolysis generates only products which are marginally soluble in hexanes and whose ^1H NMR spectra do not match those of the $1/\text{LiAlMe}_4$ reaction.

X-ray Diffraction Study of 6. The structure of **6** (Figure 5) can be viewed as a combination of an $\text{YCl}_3(\text{THF})_3$ unit with a trimetallic $\text{Y}_3(\text{OR})_3(\mu\text{-OR})_3(\mu_3\text{-OR})(\mu_3\text{-Z})\text{ZL}_2$ structure of the type previously found for yttrium *tert*-butoxides^{4,5,8,9} (see the Introduction). In **1**, $\text{Z} = \text{Cl}$ and $\text{L} = \text{THF}$ in this general formula; in **6**, the $\mu_3\text{-Z}$ is an oxide and the terminal Z ligand and the two L groups are the chloride ligands bridging from the $\text{YCl}_3(\text{THF})_3$ moiety. The two components of **6** are held together by these three bridging chlorides and by a connection between the oxide and the $\text{YCl}_3(\text{THF})_3$ unit which makes that yttrium seven-coordinate as in **5**. As a result, the oxide ligand is located within a tetrahedron of metals. The molecule has a 3-fold rotation axis such that the three yttrium atoms in the base of the tetrahedron are crystallographically equivalent as are the three chloride atoms and the three THF ligands.

The data in Table IV show that most of the metrical parameters of the $\text{Y}_3(\text{OR})_3(\mu\text{-OR})_3(\mu_3\text{-OR})(\mu_3\text{-Z})\text{ZL}_2$ base of **6** are similar to those in other trimetallic yttrium *tert*-butoxide complexes.^{4,5,31} The yttrium atoms in the base are six-coordinate as is typical for yttrium *tert*-butoxides. The 2.409(17)-Å $\text{Y}(2)\text{-O}(4)(\text{THF})$ distance in **6** is equivalent to the 2.41(1)-Å average $\text{Y-O}(\text{THF})$ distance in seven-coordinate $[\text{Y}(\text{OCMe}_3)\text{Cl}(\text{THF})_3]^+$ (**8**).³¹ The 2.778(5)-Å $\text{Y}(2)\text{-Cl}(1)$ distance is in the broad 2.681(9)–2.820(11)-Å range of distances found for six-coordinate $\text{Y}-(\mu\text{-Cl})$ connections in $\text{Y}_{14}(\text{OCMe}_3)_{28}\text{Cl}_{10}\text{O}_2(\text{THF})_4$ (**10**)⁵ and $[\text{Y}_4(\text{OCMe}_3)_{10}\text{Cl}_2\text{O}]^{2-}$ (**11**).⁴

The 2.059(23)-Å $\text{Y}(2)\text{-}\mu_4\text{-O}(5)$ distance of **6** is the shortest yttrium-oxide bond distance reported to date. It is significantly shorter than the other $\text{Y}-(\mu_4\text{-O})$ distances in the literature including the 2.13(2)–2.37(2)-Å $\text{Y}-(\mu_4\text{-O})$ distances in **10**⁵ and the 2.40(2)–2.52(2)-Å $\text{Y}-(\mu_4\text{-O})$ distances in **11**. The yttrium-oxide distances in Y_2O_3 ,⁴⁶ YVO_4 ,⁴⁷ and $\text{UO}_3\cdot 3\text{Y}_2\text{O}_3$ ⁴⁸ are also longer: 2.28, 2.443(8), and 2.305 Å, respectively.

Discussion

Facile Cleavage of the Trimetallic Unit by Trimethylaluminum. $\text{Y}_3(\text{OR})_7\text{Cl}_2(\text{THF})_2$ reacts under mild conditions with trimethylaluminum to form the monometallic complexes **2–5** (Scheme I). This reaction clearly shows that the trimetallic $\text{Y}_3(\text{OR})_3(\mu\text{-OR})_3(\mu_3\text{-OR})(\mu_3\text{-Z})\text{ZL}_2$ structure previously observed to be predominant in neutral yttrium *tert*-butoxide can be readily cleaved with the appropriate reagents. The only fully characterized yttrium *tert*-butoxide complexes previously reported in the literature which were *not* at least trimetallic were the cationic species $[\text{Y}_2(\text{OR})_4\text{Cl}(\text{THF})_4]^+$ and $[\text{Y}(\text{OR})\text{Cl}(\text{THF})_3]^+$.³¹ Although the trimetallic complex $[\text{Y}_3(\text{OR})_7\text{Cl}(\text{THF})_3]^+$ was also found in that system, it appeared that, upon formation of cationic species by reaction with the silver ion, the trimetallic unit was not as favored as in neutral complexes. Evidently, trialkylaluminum reagents will also lead to polymetallic fragmentation even in neutral species.

Although the trimetallic structure is evidently preferred for neutral yttrium and lanthanide complexes containing a ligand set comprising alkoxide, halide, and THF or alcohol, when a bridging alkylaluminum moiety is present, monometallic species are readily formed. At present, too few data are available to determine if the basis for this is (a) some aspect of the reactivity of AlMe_3 , (b) the chelating nature of the $(\mu\text{-OCMe}_3)(\mu\text{-Me})\text{AlMe}_2$ and $(\mu\text{-OCMe}_3)_2\text{AlMe}_2$ ligands in **2–4**, (c) the presence of an alkyl ligand, or (d) some other factors. Complex **4** shows that these monometallic complexes can be isolated with a single chelating ligand (which has no bridging alkyl group) even in the presence of *tert*-butoxide and chloride ligands which could bridge and two THF ligands which could dissociate to facilitate bridging. The only previous definitive studies in which polyyttrium complexes have been converted to species of lower nuclearity involved the isopropoxide complex $\text{Y}_5(\text{O-}i\text{-Pr})_{13}\text{O}$.^{6,7} This pentayttrium complex converts to monometallic $\text{Y}(\text{OSiPh}_3)_3(\text{THF})_3$ ²⁰ by treatment with Ph_3SiOH and to bimetallic $\text{Y}_2(\text{OAc})_2(\text{acac})_4(\text{H}_2\text{O})_2$ by treatment with acetylacetonone/water.^{49,50}

Synthetic Aspects. From the several products obtained from the reaction of **1** with AlMe_3 and from the structure of **4**, which shows that ligand redistribution must be occurring during the reaction, it appears that once the trimetallic starting material starts to react, several pathways are possible. Initial attack may occur by formation of a $\text{Y}(\mu\text{-Cl})(\mu\text{-Me})\text{AlMe}_2$ unit from the terminal chloride in **1**, by formation of $\text{AlMe}_3(\text{THF})$ using a THF from **1**, and/or by formation of $[(\text{Me}_3\text{CO})\text{AlMe}_3]^-$. If the last reaction occurred, this would leave a cationic residue which could fragment as observed in the reactions of Ag^+ with **1**.³¹ It is difficult to probe these details since the reaction does not occur in THF, the optimal solvent for NMR studies of these trimetallic *tert*-butoxide complexes.

This reaction provides a new option for making mixed-metal yttrium-aluminum complexes with high $\text{Al}:\text{Y}$ ratios. Although there is interest in mixed-metal yttrium- and lanthanide-aluminum compositions in areas as diverse as Ziegler-Natta catalysis⁵¹ and heavy-fermion science,⁵² previously reported synthetic routes to fully defined complexes give compounds with $\text{Al}:\text{Y}$ ratios of only 1:1 or 1:2.^{53,54}

It is important to note that we were not able to generate **2–4** from simpler starting materials. Complex **1** appears to be a crucial precursor for this reaction, and hence the trimetallic complexes of general formula $\text{Y}_3(\text{OR})_3(\mu\text{-OR})_3(\mu_3\text{-OR})(\mu_3\text{-Z})\text{ZL}_2$ may

(49) Poncellet, O.; Hubert-Pfalzgraf, L. G.; Daran, J.-C. *Polyhedron* **1990**, *9*, 1305–1310.

(50) The tetrametallic neodymium complex $[\text{Nd}(\text{O-}i\text{-Pr})_3]_4(i\text{-PrOH})_4$ forms the bimetallic complex $\text{Nd}_2(\text{OH})(\text{acac})_5$ when treated with acetylacetonone/ H_2O : Poncellet, O.; Hubert-Pfalzgraf, L. G. *Polyhedron* **1989**, *8*, 2183–2188.

(51) (a) Hattori, I.; Tsutsumi, F.; Sakakibara, M.; Makino, K. *Elastomers Plastics* **1991**, *23*, 135–151. (b) Sinn, H.; Kaminsky, W. *Adv. Organomet. Chem.* **1980**, *18*, 99. (c) *Transition Metal Catalyzed Polymerization: Ziegler-Natta and Metathesis Polymerization*; Quirk, R. P., Ed.; Cambridge University Press: New York, 1988 (and references cited therein).

(52) (a) Stewart, G. R. *Rev. Mod. Phys.* **1984**, *56*, 755–787. (b) Grewe, N.; Steglich, F. In *Handbook on the Physics and Chemistry of Rare Earths*; Gschneidner, K. A., Jr., Eyring, L., Eds.; Elsevier: Amsterdam, 1991; Vol. 14, Chapter 97.

(46) O'Conner, B. H.; Valentine, T. M. *Acta Crystallogr., Sect. B* **1969**, *B25*, 2140–2144.

(47) Baglio, J. A.; Gashurov, G. *Acta Crystallogr., Sect. B* **1968**, *B24*, 292–293.

(48) Bartram, S. F. *Inorg. Chem.* **1966**, *5*, 749–754.

provide synthetic routes unattainable in other ways. Mixed-metal lanthanum- and praseodymium-aluminum isopropoxides have previously been reported to form from $\text{LnCl}_3(\text{HO-}i\text{-Pr})_3$ and $\text{KAl}(\text{O-}i\text{-Pr})_4$, but neither NMR nor crystallographic characterization was available.⁵⁵ The nonrigid nature of **2** and **3** in solution and the apparent preference for formation of the dialuminum alkoxide, **3**, instead of the trialuminum species, **2**, raises interesting questions regarding the nature of the previously reported double alkoxides in solution.

Structural Aspects. As the first series of monometallic six-coordinate yttrium *tert*-butoxide complexes, **2–4** provide the first opportunity to consider the designed construction of a specific octahedral ligand set for an yttrium *tert*-butoxide compound. Previous yttrium *tert*-butoxide systems have shown such a strong preference to self-assemble polymetallic structures that synthetic planning had to utilize whatever polymetallic skeleton had formed. With the heavily studied cyclopentadienyl coligand systems, little flexibility is available for positioning one ligand with respect to another once two cyclopentadienyl ligands are in place. Although more data are needed to determine the ligand site preferences in these octahedral yttrium *tert*-butoxide systems, the data obtained so far suggest that planned synthesis of a specific ligand set geometry is possible.

The LiAlMe₄ Reaction. LiAlMe₄ is much less reactive with **1** than AlMe₃ and shows that facile cleavage of the trimetallic structure is not general to all alkylaluminum reagents. Upon heating, however, this reaction must also involve some cleavage of the trimetallic unit since tetrametallic species are formed from trimetallic precursors. Since this reaction occurs under more forcing conditions than those in Scheme I and since a more complicated reaction mixture is obtained, less can be said about the implications of this reaction with respect to the polymetallic fragmentation.

The most interesting aspect of this reaction involves the structure of **6**. One perspective of this structure is that it contains

(53) Most involve formation of 1:1 Ln:Al complexes in cyclopentadienyl systems: (a) Evans, W. J.; Chamberlain, L. R.; Ziller, J. W. *J. Am. Chem. Soc.* **1987**, *109*, 7209–7211. (b) Busch, M. A.; Harlow, R.; Watson, P. L. *Inorg. Chim. Acta* **1987**, *140*, 15–20. (c) Yamamoto, H.; Yasuda, H.; Yokota, K.; Nakamura, A.; Kai, Y.; Kasai, N. *Chem. Lett.* **1988**, 1963–1966. (d) Lobkovsky, E. B.; Soloveichik, G. L.; Bulychev, B. M.; Erofeev, A. B.; Gusev, A. I.; Kirillova, N. I. *J. Organomet. Chem.* **1983**, *254*, 167–172. (e) Lobkovskii, E. B.; Soloveichik, G. L.; Erofeev, A. B.; Bulychev, B. M.; Bel'skii, V. K. *J. Organomet. Chem.* **1982**, *235*, 151–159. (f) Bel'skii, V. K.; Bulychev, B. M.; Erofeev, A. B.; Soloveichik, G. L. *J. Organomet. Chem.* **1984**, *268*, 107–111. (g) Belsky, V. K.; Erofeev, A. B.; Bulychev, B. M.; Soloveichik, G. L. *J. Organomet. Chem.* **1984**, *265*, 123–133. (h) Erofeev, A. B.; Bulychev, B. M.; Bel'skii, V. K.; Soloveichik, G. L. *J. Organomet. Chem.* **1987**, *335*, 189–199. (i) den Haan, K. H.; Teuben, J. H. *J. Organomet. Chem.* **1987**, *322*, 321–329. (j) Boncella, J. M.; Andersen, R. A. *Organometallics* **1985**, *4*, 205–206. (k) den Haan, K. H.; Wielstra, Y.; Eshuis, J. J. W.; Teuben, J. H. *J. Organomet. Chem.* **1987**, *323*, 181–192. (l) Greco, A.; Bertolini, G.; Cesca, S. *Inorg. Chim. Acta* **1977**, *21*, 245–250. (m) Schaverien, C. J. *J. Chem. Soc., Chem. Commun.* **1991**, 458–460.

(54) A lanthanum analog of **2** ($\text{La}[(\mu\text{-OCMe}_3)(\mu\text{-Me})\text{AlMe}_2]_3$) has been prepared: Evans, W. J.; Golden, R. E.; Ziller, J. W. Unpublished results.

(55) (a) Mehrotra, R. C.; Agrawal, M. M. *J. Chem. Soc., Chem. Commun.* **1968**, 469–470. (b) Bradley, D. C.; Mehrotra, R. C.; Gauer, D. P. *Metal Alkoxides*; Academic Press: London, 1978; Chapter 5.

a solubilized $\text{YCl}_3(\text{THF})_3$ unit. $\text{YCl}_3(\text{THF})_3$ has low solubility even in THF. However, by attaching it to a trimetallic yttrium *tert*-butoxide framework, it has become solubilized in toluene. Moreover, it is oriented on the trimetallic framework such that all three THF ligands are in one hemisphere. To the extent that the yttrium–oxygen framework in these trimetallic complexes mimics solid-state oxides such as yttria,⁸ this complex can be viewed as a model of a solvated yttrium trichloride on yttria. This suggests that the trimetallic complexes such as **1** may be useful in converting ordinarily insoluble metal salts into soluble forms.

The structure of complex **6** can also be viewed in relationship to the tetrayttrium units in **10** and **11**. In **11**, the four yttrium atoms are located around the central $\mu_4\text{-O}$ in a butterfly arrangement rather than a tetrahedron. In **10**, one of the four yttrium atoms around the $\mu_4\text{-O}$ is displaced away from the other three yttrium atoms such that the structure is too open to describe using a four-metal geometry. Since **6** has the shortest Y–($\mu\text{-O}$) bond observed to date, it appears to be a variation on these structures which is more condensed. These three structures suggest that there is a continuum of tetrametallic $\text{Y}_4(\mu_4\text{-O})$ structures which can form in these yttrium *tert*-butoxide chloride systems. As in **10** and **11**, the origin of the oxide ligand has not been determined. Although the presence of adventitious moisture cannot be excluded, the fact that this reaction occurs in the presence of LiAlMe₄ and the fact that dialkyl ethers can be isolated from yttrium alkoxide to oxide conversions⁵⁶ suggest that the alkoxide is the source of the oxide.

Conclusion

The conversion of **1** to **2–5** by reaction with trimethylaluminum demonstrates that the trimetallic $\text{Y}_3(\text{OR})_3(\mu\text{-OR})_3(\mu_3\text{-OR})(\mu_3\text{-Z})\text{ZL}_2$ structure previously observed to be so prevalent in yttrium *tert*-butoxide complexes can be easily cleaved under mild conditions with the proper reagent. As the chemistry of the trimetallic complexes is further investigated, it is likely that additional reactions of this type will be found. This reaction provides a new route to mixed-metal yttrium–aluminum complexes as well as to a new series of octahedral yttrium *tert*-butoxide complexes. The reaction of **1** with LiAlMe₄ provides another example of trimetallic fragmentation as well as a new structural type of tetrametallic yttrium oxide complex, and this suggests a broader chemistry for the trimetallic precursor.

Acknowledgment. For support of this research, we thank the Division of Chemical Sciences, Office of Basic Energy Sciences, Department of Energy.

Supplementary Material Available: Variable-temperature NMR spectra and tables of crystal data, positional parameters, bond distances and angles, and thermal parameters (23 pages); listings of observed and calculated structure factors (24 pages). Ordering information is provided on any current masthead page.

(56) Evans, W. J.; Sollberger, M. S.; Shreeve, J. L.; Olofson, J. H.; Hain, J. H. *Inorg. Chem.* **1992**, *31*, 2492–2501.